Article:
Perutz, Robin Noel orcid.org/0000-0001-6286-0282, Jasim, Nasarella A., Whitwood, Adrian C. et al. (2 more authors) (2016) Platinum(0)-mediated C–O bond activation of ethers via an SN2 mechanism. Dalton Transactions. c6dt03241a. 18842–18850. ISSN 1477-9234

https://doi.org/10.1039/c6dt03241a

Dalton Transactions

ARTICLE

Platinum(0)-Mediated C–O Bond Activation of Ethers via S_N2 Mechanism

Received 00th January 20xx,
Accepted 00th January 20xx

DOI: 10.1039/x0xx00000x

www.rsc.org/

Manuel A. Ortuño,[a,b] Nasarella A. Jasim,[c] Adrian C. Whitwood, Agustí Lledós,*[a] and Robin N. Perutz*[c]

A computational study of the C(methyl)–O bond activation of fluorinated aryl methyl ethers by a platinum(0) complex $Pt(PCyp_3)_2$ (Cyp = cyclopentyl) (N. A. Jasim, R. N. Perutz, B. Procacci and A. C. Whitwood, *Chem. Commun.*, 2014, **50**, 3914) demonstrates that the reaction proceeds via an S_N2 mechanism. Nucleophilic attack on Pt(0) generates an ion pair consisting of a T-shaped platinum cation with an agostic interaction to a cyclopentyl group and a fluoroaryloxy anion. This ion-pair is converted to a 4-coordinate Pt(II) product *trans*-$[PtMe(OAr^F)(PCyp_3)_2]$. Structure-reactivity correlations are fully consistent with this mechanism. The Gibbs energy of activation is calculated to be substantially higher for aryl methyl ethers without fluorine substituents and higher still for alkyl methyl ethers. These conclusions are in accord with the experimental results. Further support was obtained in an experimental study of the reaction of $Pt(PCy_3)_2$ with 2,3,5,6-tetrafluoro-4-allyloxypyridine yielding the salt of the Pt(η^3-allyl) cation and the tetrafluoropyridinolate anion $[Pt(PCy_3)_2(\eta^3\text{-allyl})][OC_5NF_4]$. The calculated activation energy for this reaction is significantly lower than for fluorinated methyl ethers.

Introduction

The activation of "inert" bonds via transition-metal mediated reactions is of great interest to access high-value chemicals using simple and inexpensive substrates. The activation of C–O bonds in ethers holds promise for new synthetic pathways and, in the case of aromatic ethers, for biomass conversion.[1] Oxidative addition represents a standard class of activation process but can mask a host of different reaction mechanisms.[2]

Alkenyl and aryl ethers can be activated and used in a number of C–O cleavage reactions, especially in cross-coupling reactions,[3–6] and in catalytic hydrogenolysis.[7] However, the C–O bond cleavage of alkyl ethers remains particularly challenging despite the seminal works by Ittel and Tolman[8] and by Milstein.[9] More recently, Paneque and Carmona[10] and Goldman[11] have reported the cleavage of $C(sp^3)$–O bonds of alkyl ethers via initial C–H bond activation using Ir complexes. Goldman's studies demonstrated stoichiometric C–O activation of fluorinated methyl ethers Ar^FO–Me by reaction at Ir pincer complexes at 100 °C.[11] He followed this investigation with catalytic conversion of ethers such as 3,5-$Me_2C_6H_3O$-*i*Pr to the corresponding phenol and alkene at 150 or 200 °C (dehydroaryloxylation).[12] Intramolecular CO–alkyl cleavage at Pd(0) and Pt(0) has also been reported briefly.[13] Additionally, $C(sp^3)$–O bond activation reactions have been achieved using esters at Ir, Fe, and Pt complexes.[11,14,15]

Closely related to C–O activation is the microscopic reverse, C–O formation, reported by several authors.[16–20] Of particular significance here, is the demonstration that the reductive elimination of a $C(sp^3)$–O bond of an ether from a Pd(II) complex occurs by reversible dissociation of aryloxide anion followed by irreversible nucleophilic attack of aryloxide on cationic complex without formation of a Pd(IV) intermediate.[17c]

In this paper we follow up the recent report by some of us (Perutz *et al.*) of the activation of C(methyl)–O bonds of fluorinated arenes using $Pt(PCyp_3)_2$.[21] We demonstrated that this substrate reacts with Ar^FO–Me to form *trans*-$[PtMe(OAr^F)(PCyp_3)_2]$ (Scheme 1). Notable features of these reactions were selectivity for cleavage of the O–CH_3 bond, an increased rate in THF compared to hexane, a negligible kinetic isotope effect for replacement of the OCH_3 group by OCD_3, a reduction in rate with fewer fluorine substituents, and the absence of reaction with anisole itself. The reaction proceeded at 60° C over 2 days in hexane with 1 equiv. of substrate (pentafluoroanisole or 4-methoxytetrafluoropyridine) but at room temperature with 10 equiv. substrate. We concluded that a phosphine-assisted mechanism was possible, but a nucleophilic attack mechanism via an ion-pair $[PtMe(P(Cyp)_3)_2]^+[Ar^FO]^-$ was most likely considering the study of C–O reductive elimination[17c] at Pd and evidence for analogous three-coordinate Pt cations.[22,23] Here we make use

[a] Departament de Química, Centro de Innovación en Química Avanzada (ORFEO-CINQA), Universitat Autònoma de Barcelona, 08193 Cerdanyola del Vallès, Spain.
[b] Department of Chemistry, Chemical Theory Center, and Supercomputing Institute, University of Minnesota, Minneapolis, Minnesota 55455, USA.
[c] Department of Chemistry, University of York, York YO10 5DD, UK.

† Electronic Supplementary Information (ESI) available: Experimental and computational structural parameters, DFT-optimised structures of THF complexes, XYZ coordinates and energies, spectra of 2,3,5,6-tetrafluoro-4-allyloxypyridine and $[Pt(PCy_3)_2(\eta^3\text{-allyl})][OC_5NF_4]$. See DOI: 10.1039/x0xx00000x

of the experience of the rest of our team (Ortuño and Lledós) in understanding three-coordinate platinum cations to investigate the mechanisms of these reactions by computational methods.[23–25]

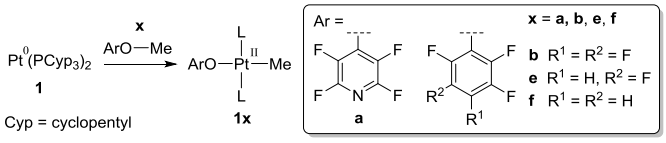

Scheme 1 C(methyl)–O bond activation of fluorinated arenes at a Pt(0) centre.

We demonstrate that the C(methyl)–O activation does indeed proceed by an S_N2 mechanism involving an ion-pair and support these conclusions with structure–reactivity correlations. In addition, we report the reaction of $Pt(PCy_3)_2$ with an allyl ether and show that the product is a salt analogous to the ion-pair above, thus supporting the S_N2 mechanism.

Results and discussion

Computational study of C–O bond activation mechanism

The C–O bond activation mechanism for the representative reaction between $Pt(PCyp_3)_2$ **1** and pentafluoroanisole **b** in THF (Scheme 2) has been investigated at the DFT level using the M06 functional (see Computational details). Two pathways have been explored, namely, concerted oxidative addition (OA) and bimolecular nucleophilic substitution (S_N2).[26,27] Since no experimental evidence of Pt(I) dimers was found, we initially ruled out a single-electron transfer mechanism.[28] All energies reported are Gibbs energies in THF in kcal mol^{-1} and are reported relative to the separated species **1** + **b**.

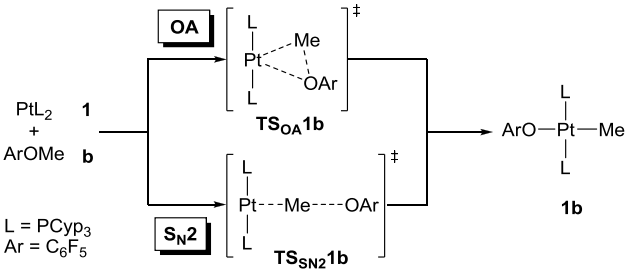

Scheme 2 Proposed reaction mechanisms for the formation of **1b**.

The computed Gibbs energy profile of the reaction between **1** and **b** is shown in Fig. 1. Initially, different interaction modes between the substrate **b** and the bis-ligated complex **1** have been considered. As expected for an electron-rich Pt(0) centre, no stable η^1-O coordination modes are located; instead, the van der Waals complex **1·b** is found at 4.9 kcal mol^{-1}. The angle P–Pt–P remains almost linear (171.6°), but the long Pt···H_{Me} distance (2.929 Å) precludes its description as a σ-complex (Fig. 2a). The C(methyl)–O bond distance is 1.438 Å, essentially equal to the value for the free substrate **b** (1.435 Å). A η^2-CC coordination mode via the aryl group, **1·b-CC**, is found at higher energy (16.2 kcal mol^{-1}), likely due to the strong distortion of the linear P–Pt–P arrangement (113.7°, Fig. 2a). This casts doubt on the assignment of the species as **1·b-CC** that we observed on following the reaction with pentafluoranisole by NMR spectroscopy, as we suggested in ref 20.

Starting from **1·b**, two pathways for the C(methyl)–O bond cleavage have been calculated. On the one hand, the concerted oxidative addition route (OA) involves an activation energy of 53.9 kcal mol^{-1} via $\mathbf{TS_{OA}1b}$, giving rise to the square-planar Pt(II) product **1b** at −10.0 kcal mol^{-1}. $\mathbf{TS_{OA}1b}$ shows a three-membered Pt-C-O ring with a C(methyl)···O distance of 2.012 Å (Fig. 2b). However, the transition state structure lies high in energy and this route is clearly inaccessible. Then, by analogy with Pd(0) chemistry, the feasibility of mono-phosphine species has been computationally evaluated.[29,30] One phosphine ligand in **1** has been replaced by the substrate **b** which coordinates to Pt via η^1-O mode forming $\mathbf{1_Lb}$. This intermediate is found at 33.6 kcal mol^{-1}; since this energy is considerably higher than that for the mechanism described below, this route can also be ruled out. On the other hand, a nucleophilic substitution (S_N2) transition state $\mathbf{TS_{SN2}1b}$ allows the reaction to proceed, demanding an energy only 27.4 kcal mol^{-1} above reactants. The S_N2 nature is evident from the planar disposition of the C-methyl substituent, with the Pt(0) complex being the nucleophile and the $C_6F_5O^-$ anion the leaving group (Pt–C–O angle of 175.4°).[31] The forming Pt···C(methyl) and breaking C(methyl)···O distances in $\mathbf{TS_{SN2}1b}$ are 2.497 Å (2.929 Å in **1·b**) and 1.929 Å (1.438 Å in **1·b**), respectively (Fig. 2b). The species directly formed from $\mathbf{TS_{SN2}1b}$ is the ion-pair **1b·OAr** at 5.0 kcal mol^{-1} which presents a low-coordinate Pt(II) centre,[23] stabilised by a δ-agostic interaction with the Cyp group of the phosphine ligand. The Pt···H_{ag} and Pt···C_{ag} distances are 2.090 Å and 3.049 Å, respectively, similar to other agostic interactions.[23,32,33] No evidence of such agostic contact is found in $\mathbf{TS_{SN2}1b}$, which shows Pt···H_{ag} and Pt···C_{ag} distances of 3.620 and 4.197 Å, respectively. The corresponding cationic complex **1b+** (formed by removing the $C_6F_5O^-$ anion from **1b·OAr**) is located at 2.9 kcal mol^{-1} and preserves the δ-agostic interaction (Pt···H_{ag} = 2.067 Å, Pt···C_{ag} = 3.029 Å, Fig. 2c).[34] An alternative conformer displaying a γ-agostic interaction, **1b+'**, is found at 6.0 kcal mol^{-1} with similar structural parameters (Pt···H_{ag} = 2.207 Å, Pt···C_{ag} = 3.063 Å, Fig. 2c). Since the Gibbs energy difference between **1b+** and **1b+'** is ca. 3 kcal mol^{-1}, both γ- and δ-agostic modes may be accessible in solution.[23,25,33] Finally, the anion eventually reorganises to bind to the Pt centre yielding the neutral four-coordinate square-planar product **1b** (Scheme 2, Table S1).

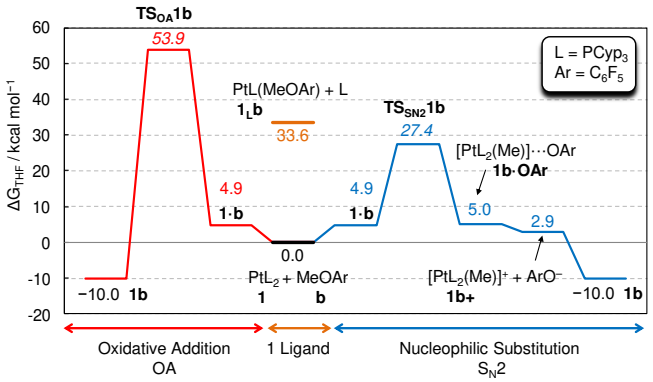

Fig. 1 Gibbs energy profile for the formation of **1b**.

According to the S_N2 mechanism, a vacant coordination site at Pt in **1b·OAr** is readily produced after the C–O bond breaking. Since THF may coordinate to low-coordinate Pt centres,[23,25,35] the role of one molecule of THF stabilising the nascent vacancy has been evaluated. One molecule is explicitly included in both the reactant and the S_N2 transition state structures, i.e., **1·THF** and **TS_{SN2}1b·THF** (Fig. S1). The Pt···O_{THF} distances are 4.035 and 4.109 Å, respectively, and the corresponding Gibbs activation energy is 28.1 kcal mol^{-1}, which shows no significant difference from the counterpart with THF absent (27.4 kcal mol^{-1} via **1** and **TS_{SN2}1b**). Thus, no active role can be unambiguously assigned to solvent molecules during the C–O bond activation process. Interestingly, the reaction of **1** with **b** can also be performed in hexane, although the half-life of **1** was ca. 3 times shorter in THF than in hexane.[21] According to the previous calculations, that observation can be merely related to the higher dielectric constant of THF (ε = 7.426) with respect to hexane (ε = 1.882) which favours the charge separation via S_N2 mechanism.

An alternative proposed previously involved a phosphine-assisted mechanism as has been observed in the reaction of $Pt(PCy_3)_2$ with pentafluoropyridine.[21,36] The closest phosphorus in **TS_{OA}1b** appears far away from the oxygen atom at 3.565 Å, thus precluding any significant interaction. Also, since we could not find a minimum structure for the complex $[Pt(PCyp_3)(ArO–PCyp_3)(Me)]$, this pathway has been ruled out.

Overall, the computational picture favours the bimolecular nucleophilic substitution over oxidative addition. This mechanism can also explain the lack of C(aryl)–O bond activation since MeO^- is a poorer leaving group than ArO^-.

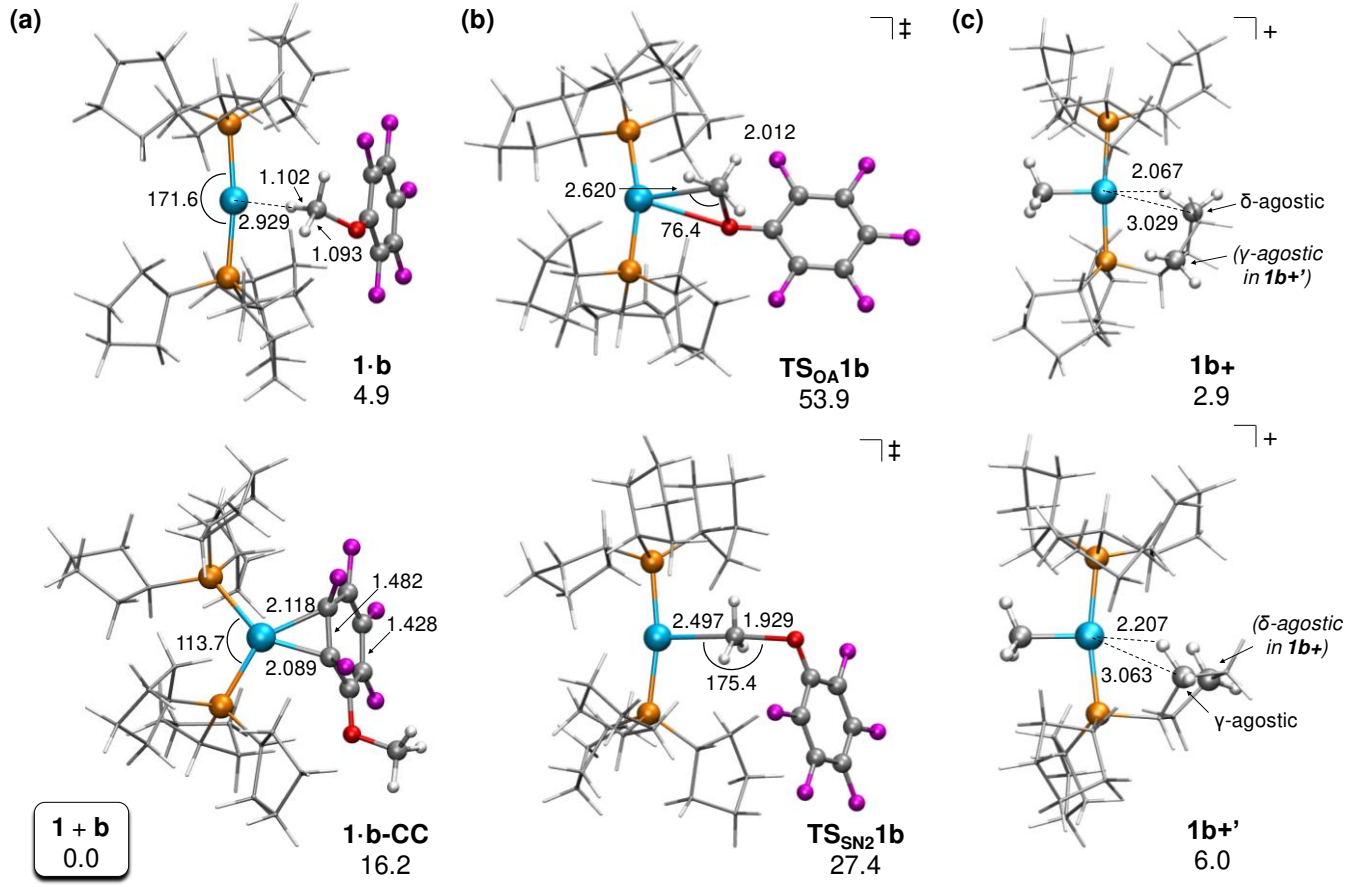

Fig. 2 DFT-optimised structures of *(a)* reactants **1·b** and **1·b-CC**, *(b)* transition states **TS_{OA}1b** and **TS_{SN2}1b**, and *(c)* agostic intermediates **1b+** and **1b+'**. Distances in Å and angles in degrees. Gibbs energies in THF in kcal mol^{-1}.

C–O bond activation of other substrates

In this section we study the C–O bond activation for different substrates (see below). According to the previous results, only the S_N2 mechanism is considered. All Gibbs energies are reported in THF in kcal mol^{-1} and are related to the separated species **1** and substrate.

For the sake of comparison and further analysis, the S_N2 mechanism has been computed for different methoxy-based substrates as reported experimentally,[21] i.e., **a**, **e**, **f**, and **an** (Scheme 3a). The van der Waals complexes **1·a**, **1·e**, **1·f** and **1·an** are energetically similar to **1·b**, in the range of 3–6 kcal mol^{-1}. The corresponding transition states **TS_{SN2}1a**, **TS_{SN2}1e**, **TS_{SN2}1f**, and **TS_{SN2}1an** are found at 26.1, 27.9, 27.2, and 38.7

kcal mol^{-1}, respectively; the products **1a**, **1e**, **1f**, and **1an** at −13.8, −9.2, −7.0, and −0.8 kcal mol^{-1}, respectively (Table S1). This trend shows that the presence of fluorine atoms in the aryl group both decreases the activation free energy and stabilizes the final product. These results are in broad agreement with previous experiments, which showed a reaction with **a**, **b**, **e** and **f** whereas **1-an** was not reactive.[21] However, the calculated barriers for **b**, **e** and **f** are not significantly different from one another, while the experimental order of reactivity was **b** > **e** > **f**.

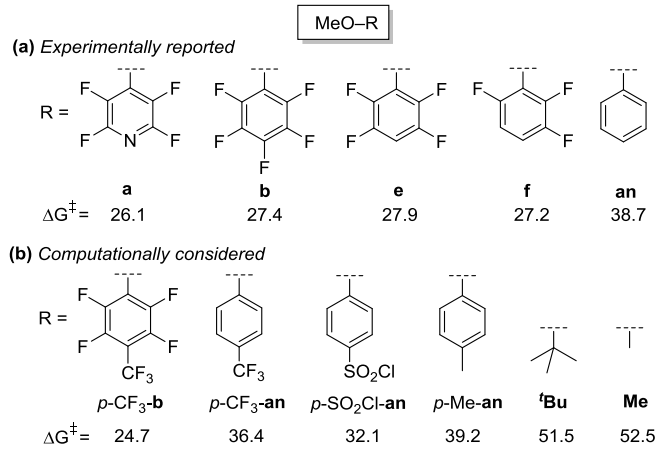

Scheme 3 Substrates under study and their corresponding Gibbs activation energies via S_N2 mechanism (kcal mol^{-1}).

To obtain better insight into the influence of the groups of the aryl moiety, the computational study has been extended to other substrates not reported experimentally (Scheme 3b). Initially, **b** has been modified by including the electron-withdrawing group CF_3 in *para* position, *p*-CF_3-**b**. This change results in a Gibbs activation energy of 24.7 kcal mol^{-1}, 1.4 kcal mol^{-1} lower than that for **b**. Analogously, **an** has been tuned with the electron-withdrawing groups CF_3 and SO_2Cl, *p*-CF_3-**an** and *p*-SO_2Cl-**an**, and the electron-donating group CH_3, *p*-Me-**an**. In comparison to **an** (38.7 kcal mol^{-1}), the former electron-withdrawing groups decrease the activation energy (32–36 kcal mol^{-1}) where the latter electron-donating group slightly increases it (39.2 kcal mol^{-1}). Finally, the aryl moiety has been substituted by the alkyl groups, **^{t}Bu** and **Me**. Unsurprisingly, both of them display large Gibbs activation energies, ca. 52 kcal mol^{-1}, since alkoxy moieties are known to be poor leaving groups. The computed trend suggests that substrates with electron-withdrawing groups, i.e. capable of delocalising the incipient negative charge of the oxygen atom, are more suitable to undergo C–O bond activation via the S_N2 mechanism. These results will be discussed in next section.

Structure–reactivity correlations

Previous calculations have shown the major influence of the substituents of the aryl leaving group in the S_N2 reaction mechanism (Scheme 3). In this section, correlations between structural parameters and Gibbs activation energies will be closely inspected for the previously computed methoxy ethers (**x** = **a**, **b**, **e**, **f**, **an**, *p*-CF_3-**b**, *p*-CF_3-**an**, *p*-SO_2Cl-**an**, *p*-Me-**an**, **^{t}Bu**, **Me;** Scheme 3).

Fig. 3 plots the C···O vs. Pt···C distances of the transition state structures **TS_{SN2}1x**. The data were fitted by linear regression (R^2 = 0.981) yielding a negative slope, meaning that short C···O distances correlate to longer Pt···C distances and vice versa. Such behaviour is fully consistent with the hyperbolic reaction coordinates set out by Bürgi and Dunitz.[37]

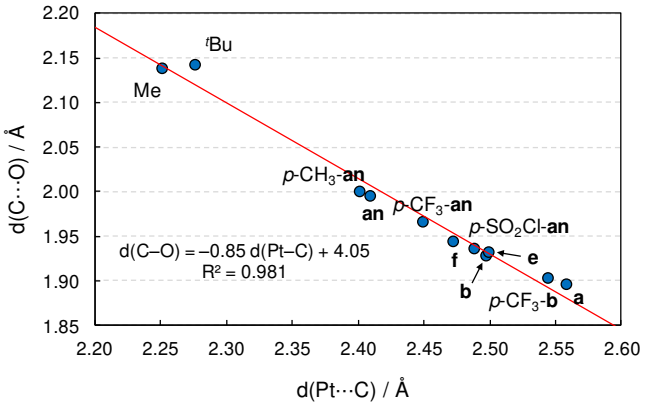

Fig. 3 Plot of C···O vs. Pt···C distances of **TS_{SN2}1x**. Regression line in red.

Structure–reactivity relationships are now inspected. Fig. 4 plots Gibbs activation energy against C···O and Pt···C distances of **TS_{SN2}1x**. Moderate correlation coefficients are found for both parameters (R^2 ca. 0.95), indicating that shorter C···O and longer Pt···C distances (i.e., reactant-like transition states) correlate with lower Gibbs activation energies.

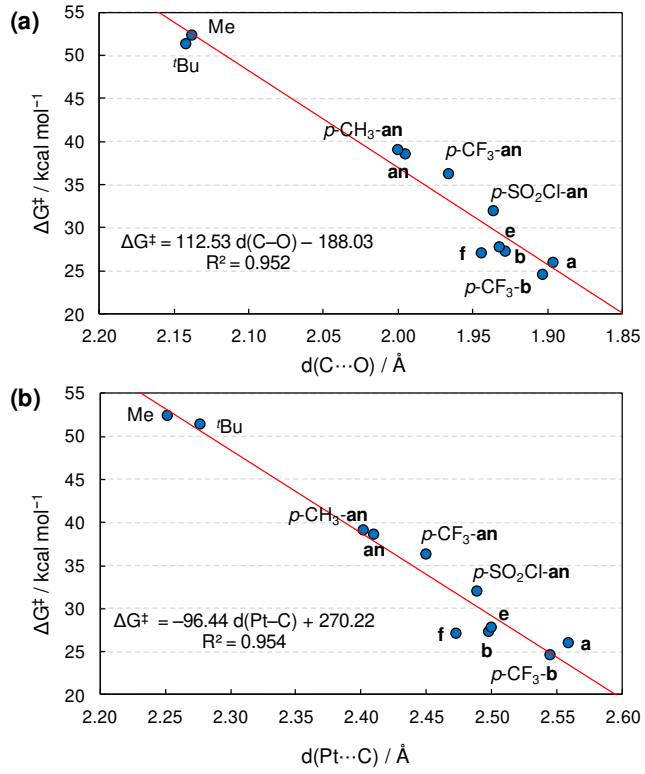

Fig. 4 Plots of Gibbs activation energies vs. *(a)* C···O and *(b)* Pt···C distances of **TS_{SN2}1x**. Regression lines in red.

The nature of the leaving group is of great importance in S_N2 reactions.[38] Here we focus on the ability of the RO groups to stabilise the incoming negative charge. The charge of the oxygen atom of the isolated anion RO^-, q(O), has been plotted against its corresponding activation free energy in Fig. 5. The overall distribution indicates that the lower the absolute value of q(O), the lower the Gibbs activation energy. In other words, the delocalisation of the negative charge of the oxygen over the group R facilitates the reaction. The poorer correlation coefficient for the linear regression (R^2 = 0.881) compared to those in Fig. 3 and 4 may be related to the simplicity of q(O) as a global descriptor, since other important stereo-electronic contributions present in the transition states, including conformational diversity, cannot be fully captured. If the set of strong electron-deficient F-containing derivatives is removed (**a**, **b**, **e**, **f**, and *p*-CF_3-**b**), a better fit is achieved (R^2 = 0.972, Fig. S2).

To sum up, good correlations between energies and distances in transition states were found for different leaving groups (Fig. 4). The simple and intuitive q(O) descriptor can also, be used to predict the reactivity of substrates (Fig. 5).

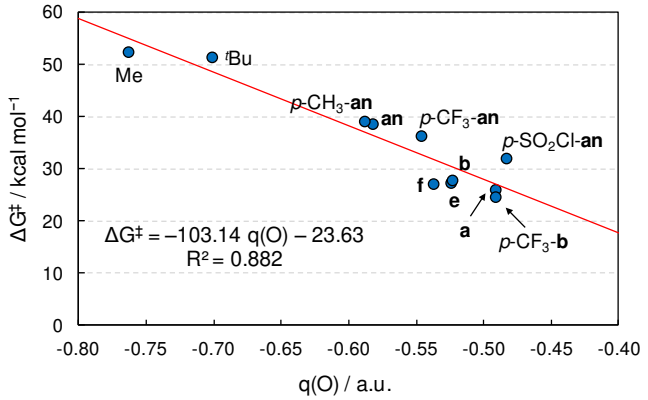

Fig. 5 Plot of Gibbs activation energy vs. q(O) of $\mathbf{TS_{SN2}1x}$. Regression line in red.

Experimental and computational reactivity toward 2,3,5,6-tetrafluoro-4-allyloxypyridine

The study that we reported previously was fully consistent with a mechanism involving nucleophilic attack of $Pt(PCyp_3)_2$ at the C–O bond of the fluorinated pyridine derivative or fluorinated benzene derivative.[21] This conclusion has been vindicated by the computational results described in this paper. In order to find further experimental evidence, we decided to investigate a related allyloxy compound, anticipating that cleavage of an O-allyl bond should be more facile than cleavage of the O-methyl bond. The 4-substituted tetrafluoropyridine, 2,3,5,6-tetrafluoro-4-allyloxypyridine, was synthesised by slow addition of a THF solution of $NaOCH_2$–$CH{=}CH_2$ to pentafluoropyridine. This method avoids formation of doubly substituted pyridines. The reaction of the resulting 2,3,5,6-tetrafluoro-4-allyloxypyridine **g** (1 equiv.) with $Pt(PCy_3)_2$ **2** in hexane proceeded immediately at room temperature forming a colourless precipitate that was recrystallised from benzene/hexane to yield **2g**. Notably, this reaction proceeds much faster than any of those described in ref 21. The molecular structure of **2g** was determined by X-ray crystallography as the salt of tetrafluoropyridinolate $[Pt(PCy_3)_2(\eta^3\text{-allyl})][OC_5NF_4]$ (Fig. 6). The bond lengths and angles of the $[Pt(PCy_3)_2(\eta^3\text{-allyl})]$ cation are consistent with those in the crystal structure of the PF_6^- salt recorded at room temperature, including the disorder in the allyl group.[39] The tetrafluoropyridinolate anion exhibits a C–O bond length of 1.249 (3) Å which compares to the literature value of 1.292 (7) Å in the structure of $[Et_2NH_2][C_5NF_4O]$ where the oxygen atom is hydrogen-bonded to two cations,[40] 1.280(2) Å in $\{[K(H_2O)][C_5NF_4O]\}_n$,[41] and 1.281 (2) when coordinated to palladium in $Pd(CH_3)(OC_5NF_4)(Me_2NCH_2CH_2NMe_2)$.[42]

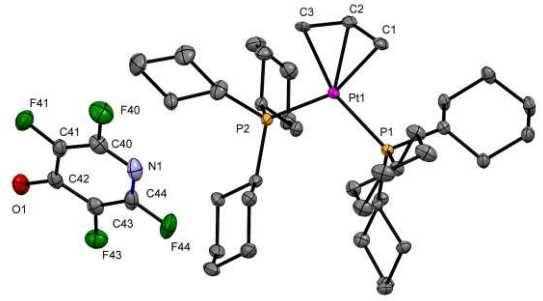

Fig. 6 Molecular structure of $[Pt(PCy_3)_2(\eta^3\text{-allyl})][OC_5NF_4]$ **2g**. The allyl group is disordered over two positions, but only one is shown. Hydrogen atoms are omitted and anisotropic displacement parameters are shown as 50% ellipsoids. Principal bond lengths (Å) and angles (°): Cation Pt–P(1) 2.3329(6), Pt–P(2) 2.3309(6), Pt–C(1) 2.201(2), Pt–C(2) 2.157(4), Pt–C3 2.183(8), P(1)–Pt–P(2) 112.84(2), C(1)–C(2)–C(3) 121.7(5), C(1)–Pt–C(3) 67.3(2); Anion C(42)–O(1) 1.249(3), C(40)–N(1) 1.316(4), C(44)–N(1) 1.313(4).

The ^1H, ^{31}P, and ^{13}C NMR spectra of CD_2Cl_2 solutions of **2g** were fully consistent with literature spectra of $[Pt(PCy_3)_2(\eta^3\text{-allyl})]^+$, previously recorded as the PF_6^- salt.[43,44] In addition, we supported the assignment with ^1H-^{31}P and ^1H-^{13}C HMQC spectra, a ^{195}Pt spectrum which showed a triplet at δ −5285 (J(PtP) 3804 Hz) and ^1H-^{195}Pt HMQC spectra. The tetrafluoropyridinolate anion exhibited two resonances in the ^{19}F NMR spectra and three resonances with ^{19}F coupling in the ^{13}C NMR spectra (see Experimental section). It is significant that the complex is only slightly soluble in benzene unlike the neutral Pt complexes described in ref 21. There is no evidence for formation of a neutral complex in solution with coordinated tetrafluoropyridinolate as has been observed previously with a palladium complex.[42] The activation of allyl ethers may be compared to the reactions of methyl allyl ether and diallyl ether at Fe centres to form allyl complexes.[14]

In line with previous calculations, we have computed the C(allyl)–O bond activation of the 4-allyloxy-tetrafluoropyridine **g** using the derivative $Pt(PCyp_3)_2$ **1**.[45] First, the van der Waals complex **1·g** is found at 5.1 kcal mol^{-1}, which is similar to **1·b** (4.9 kcal mol^{-1}). The S_N2 transition state $\mathbf{TS_{SN2}1g}$ is located at 22.2 kcal mol^{-1} above reactants. The resulting ion-pair **1g·OAr** at −1.1 kcal mol^{-1} exhibits a η^1 mode for the allyl moiety. However, the allyl ligand can change its coordination mode from η^1 to η^3 to form the more stable species **1g'·OAr** located at −12.7 kcal mol^{-1} (Fig. 7). The computed bond lengths and

angles are in good agreement with the experimental values. The calculated Gibbs activation energy is even lower than those for **a** or *p*-CF_3-**b** in keeping with the allylic effect on S_N2 reactions. Recently this reduction in barrier has been attributed to electrostatic interactions in the transition state rather than π-conjugation.[46]

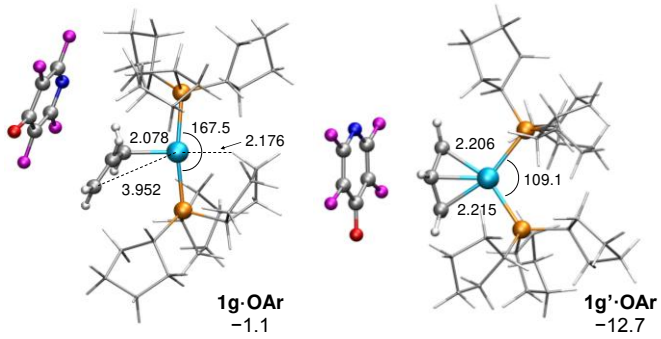

Fig. 7 DFT-optimised structures of **1g·OAr** and **1g'·OAr**. Distances in Å and angles in degrees. Gibbs energies in THF in kcal mol^{-1}.

Conclusions

This computational study, when taken with the previously published experimental evidence, establishes that the reaction of $Pt(PCyp_3)_2$ with fluorinated aryl methyl ethers proceeds via nucleophilic attack of the platinum(0) complex on the ether generating a T-shaped cation with an agostic interaction with a cyclopentyl group. With the substrates examined previously, the OAr^- anion attacks to form the final four-coordinate Pt(II) product. The calculated Gibbs activation energies for the substrates considered experimentally are in the range 26-28 kcal mol^{-1}. The calculated Gibbs activation energies for other substrates were all substantially higher with the exception of 2,3,5,6-tetrafluoro-4-trifluoromethylanisole. The S_N2 mechanism was also supported by the correlation between C···O and Pt···C distances in the transition state. As expected, the Gibbs activation energy correlated with both the C···O and Pt···C distances in the transition state. There was a weaker correlation between Gibbs activation energies and the charge on oxygen of the leaving group.

Further support was obtained in an experimental study of the reaction of $Pt(PCy_3)_2$ with 2,3,5,6-tetrafluoro-4-allyloxypyridine which yields the salt of the well-known $Pt(\eta^3$-allyl) cation and a pyridinolate anion $[Pt(PCy_3)_2(\eta^3$-allyl)$][OC_5NF_4]$ which has been fully characterised. The reaction is considerably faster than that of $Pt(PCyp_3)_2$ with methoxytetrafluoropyridine. A computational study of this reaction using $Pt(PCyp_3)_2$ demonstrates that the activation energy for this nucleophilic attack of the 2,3,5,6-tetrafluoro-4-allyloxypyridine is ca. 4 kcal mol^{-1} lower than that for 2,3,5,6-tetrafluoro-4-methoxypyridine, consistent with a significant allyl effect.

The conclusion that these C–O activation reactions proceed via nucleophilic attack is fully consistent with previous studies on reductive elimination from related palladium complexes[17c] and on T-shaped platinum complexes.[22–25] On the other hand, it differs from the reactions of fluorinated aryl methyl ethers at iridium pincer complexes that involve initial C–H bond activation.[11]

Computational details

All calculations were performed at the DFT level[47] using the M06 functional[48] with an ultrafine grid[49] as implemented in Gaussian09.[50] This functional accounts for dispersion interactions and has a good performance on organometallic systems.[51] The Pt atom was described by means of an effective core potential SDD for the inner electron and its associated double-ζ basis set for the outer ones,[52] complemented with a set of f-polarisation function.[53] The 6-31G** basis set was used for the H, N, C, O, F, P, S, and Cl atoms.[54] Diffuse functions were added for O, F, and Cl atoms.[55] All intermediates and transition states were fully optimised in tetrahydrofuran solution (THF, ε = 7.426) using the continuum method SMD.[56] Transition states were identified by having one imaginary frequency in the Hessian matrix. It was confirmed that transition states connect with the corresponding intermediates by means of application of an eigenvector corresponding to the imaginary frequency and subsequent optimisation of the resulting structures. All energy values correspond to Gibbs energies in THF in kcal mol^{-1}. Charges were computed using the CM5 model.[57]

Experimental section

General Procedures

All operations were performed under an argon atmosphere, either on a high-vacuum line (10^{-4} mbar) using modified Schlenk techniques, on standard Schlenk (10^{-2} mbar) lines or in a glovebox. Solvents for general use (hexane, benzene) were of AR grade, dried by distillation over standard reagents, or with a solvent purification system, and stored under Ar in ampoules fitted with Young's PTFE stopcocks. Deuterated solvents were dried by stirring over potassium, and were distilled under high vacuum into small ampoules with potassium mirrors.

Tricyclohexylphosphine was purchased from Strem. Pentafluoropyridine and allyl alcohol were purchased from Sigma-Aldrich. The NMR spectra were recorded on Bruker AMX500 spectrometers (^{1}H 500.13, ^{31}P 202.46, ^{19}F 407.4, ^{13}C 125.75, ^{195}Pt 107.52 MHz). The ^{1}H NMR chemical shifts were referenced to residual C_6D_5H at δ 7.15. The ^{31}P{1H} NMR spectra are reported downfield of an external solution of H_3PO_4 (85%). The ^{19}F NMR spectra were referenced to external C_6F_6 at δ −162.9. The ^{195}Pt spectra were referenced relative to the absolute frequency of 86.024 MHz as δ 0. LIFDI mass spectra were measured on a Waters Micromass GCT Premier orthogonal time-of-flight instrument set to one scan per second with resolution power of 6000 fwhm and equipped with a LIFDI probe from LINDEN GmbH.[58] Elemental analyses were performed by Elemental Microanalysis Ltd, Devon, UK. The complex $Pt(PCy_3)_2$ was synthesized by published methods.[59]

Diffraction data for **1b** were collected at 110 K on an Agilent SuperNova diffractometer with MoKα radiation (λ = 0.71073 Å). Data collection, unit cell determination and frame integration were carried out with "CrysalisPro". Absorption corrections were applied using crystal face-indexing and the ABSPACK absorption correction software within CrysalisPro. The structure was solved and refined using Olex2[60] implementing SHELX algorithms.[61] The allyl ligand was disordered and modelled in two positions with equal occupancy. The allylic hydrogens were located by difference map and allowed to refine. However, the terminal CH_2 C-H bond lengths were restrained to be equal.

Empirical formula, $C_{44}H_{71}F_4NOP_2Pt$; Formula weight, 963.04; *T*, 110.05(10) K; monoclinic, $P2_1/n$; a = 15.67024(20), b = 17.60500(17), c = 16.44506(19) Å, β = 110.4669(14)°; V = 4250.39(9) Å^3; Z = 4; ρ_{calc} = 1.505 g cm^{-3}; μ = 3.428 mm^{-1}; $F(000)$ = 1976.0; crystal size 0.2442 × 0.1984 × 0.0915 mm^3; radiation, MoKα, 0.71073 nm; 2θ range, 6.014 to 60.06°; index ranges , -22 ≤ h ≤ 15, -24 ≤ k ≤ 22, -17 ≤ l ≤ 23; reflns collected 21764; ind reflns 12386 [R_{int} = 0.0249, R_{sigma} = 0.0413]; data/restraints/parameters 12386/28/520; goodness-of-fit on F^2 = 1.041; final R [I>=2σ (I)], R_1 = 0.0251, wR_2 = 0.0508; final R [all data], R_1 = 0.0346, wR_2 = 0.0549; largest diff. peak/hole 1.05/-0.73 e Å^{-3}.

Syntheses

Synthesis of 2,3,5,6-tetrafluoro-4-allyloxypyridine. Sodium (0.4 g, 0.0174 mmol) was sliced and added to THF solution of allyl alcohol (1 g, 0.0172 mmol). The reaction was left for 2 h until all the sodium had reacted. The sodium oxyallyl was added dropwise to pentafluoropyridine (2 g, 0.0172 mmol) . at 0° C. The mixture was stirred for a few minutes and then heated at 60 °C for 1 h. THF was removed under vacuum and the product was extracted with ether, then washed with water and brine. The ether layer was collected and dried over magnesium sulfate. The solution was filtered and ether was removed under vacuum to give the product as a colourless liquid.

Mass spec: LIFDI, M+. Calcd for $C_8H_5F_4NO$ 207.03 (100%) and 208.03 (8%). Experimental isotope pattern: 207.03 (100%) and 208.03 (18%).

^{1}H NMR (C_6D_6) δ 5.48 (ddtt, 17.2, 10.4, 5.7, J(HF) 0.5 Hz, 1H, C*H*=CH_2), 5.00 (d of app quartets, 17.4, 1.4 Hz, 1H CH=CH*H*), 4.89 (d of app quartets, 10.4, 1.2 Hz), 1H, CH=C*H*H), 4.18 (d of app quintets, 5.8, 1.5 Hz, 2H).

^{19}F NMR (C_6D_6) δ-91.4 (m, 2F) -158.8 (m, 2F).

^{13}C{^{1}H} NMR (C_6D_6) δ 73.8 (t, J(CF) 4.4 Hz, *C*H_2), 119.1 (s, CH=*C*H_2), 131.1 (t, J(CF) 1.1 Hz, *C*H=CH_2), 134 (dm ^1J(CF) 256 Hz, CF), 144.1 (dm ^1J(CF) 240 Hz, CF), 146.1 (m, CO).

Synthesis of [Pt(PCy$_3$)$_2$(η^3-allyl)][OC$_5$NF$_4$]. 2,3,5,6-tetrafluoro-4-allyloxypyridine (3 mg, 0.0144 mmol) was added into a J Young's NMR tube at room temperature containing a pale yellow hexane solution of $Pt^0(PCy_3)_2$ (Cy = cyclohexyl) (10 mg, 0.0132 mmol). A colourless precipitate formed immediately and was recrystallised from benzene/hexane to give colourless crystals of complex [Pt(PCy$_3$)$_2$(η^3-allyl)][OC$_5$NF$_4$].

Mass spec: LIFDI, M^+ Calcd isotope pattern for $C_{39}H_{72}P_2Pt$: 795.47 (76%), 796.47 (100%), 797.47 (90%), 798.47 (20%), 799.47 (2%), 800.47 (12%). Experimental isotope pattern: 795.43 (71%), 796.43 (100%), 797.47 (86%), 798.45 (86%), 799.44 (20%), 800.47 (8%)

CHN analysis: Calcd. C 54.87, H 7.43, N 1.45; Found C 54.72, H 7.37, N 1.49.

^{1}H NMR (CD_2Cl_2) δ 1.34 – 1.9 (63 H, cyclohexyl), 2.34 (m, 3 H, cyclohexyl), 2.48 (m, 2 H, allyl H_{anti}), 4.38 (br, 2H allyl H_{syn}), 4.89 (m, 1H, allyl $H_{central}$).

^{31}P{^{1}H} (CD_2Cl_2) δ 27.8 (s, J(PtP) = 3780 Hz).

^{195}Pt{^{1}H} (CD_2Cl_2) δ −5285 (t, J(PtP) 3804 Hz).

^{19}F (CD_2Cl_2) δ −104.4 (m, F *ortho* to N), −174.1 (m, F *meta* to N).

^{13}C{^{1}H} (CD_2Cl_2) δ 26.1 (s, cyclohexyl, CH_2), 27.9 (m, cyclohexyl CH_2), 30.5 (d J(CP) 10, ^1J(PtC) 28 Hz, cyclohexyl CH_2), 37.3 (b, cyclohexyl CH), 61.9 (ABX pattern with Pt satellites, |$^2J(PC)_{cis}$ + $^2J(PC)_{trans}$| 28.4 Hz, ^1J(PtC) 17.4 Hz, allyl central C), 113.4 (t J(PC) 2.5, J(PtC) 17.4 Hz, allyl CH), δ 136.6 (dm, ^1J(CF) = 239 Hz, $C_5NF_4O^-$), δ 145.5 (dm, ^1J(CF) 229 Hz, $C_5NF_4O^-$), δ 160.5 (t, ^2J(CF) 7 Hz, $C_5NF_4O^-$).

Acknowledgements

Financial support from the Spanish Ministerio de Economia y Competitividad (project CTQ2014-54071-P) is gratefully acknowledged.

Notes and references

1 J. Zazeski, P. C. A. Bruijnincx, A. L. Jongerius and B. M. Weckhuysen, *Chem. Rev.,* 2010, **110**, 3552.

2 M. Crespo, M. Martínez, S. M. Nabavizadeh, M. Rashidi, Coord Chem. Rev., 2014, **279**, 115.

3 *(a)* D.-G. Yu, B.-J. Li and Z.-J. Shi, *Acc. Chem. Res.*, 2010, **43**, 1486; *(b)* J. Cornella, C. Zarate and R. Martin, *Chem. Soc. Rev.*, 2014, **43**, 8081.

4 B N. Rosen, K. W. Quasdorf, D. A. Wilson, N. Zhang, A.-M. Resmarita, N. K. Garg and V. Percec, *Chem. Rev.,* 2011, **111**, 1346.

5 *(a)* M. Tobisu, T. Takahira, T. Morioka and N. Chatani, *J. Am. Chem. Soc.,* 2016, **138**, 6711; *(b)* Tobisu, M.; Chatani, N. *Acc. Chem. Res.,* 2015, **48**, 1717.

6 *(a)* F. Kakiuchi, M. Usui, S. Ueno, N. Chatani and S. Murai, *J. Am. Chem. Soc.,* 2004, **126**, 2706; *(b)* S. Ueno, E. Mizushima, N. Chatani and F Kakiuchi, *J. Am. Chem. Soc.,* 2006, **128**, 16516; (c) M. J. Iglesias, A. Prieto and M. C. Nicasio, *Org. Lett.,* 2012, **14**, 4318.

7 *(a)* A. G. Sergeev and J. F. Hartwig, *Science,* 2011, **332**, 439; *(b)* A. G. Sergeev, J. D. Webb and J. F. Hartwig, *J. Am. Chem. Soc.,* 2012, **134**, 20226; *(c)* L. Xu, L. W. Chung and Y.-D. Wu *ACS Catal.*, 2016, **6**, 483.

8 *(a)* S. D. Ittel, C. A. Tolman, A. D. English and J. P. Jesson, *J. Am. Chem. Soc.*, 1978, **100**, 7577; *(b)* C. A. Tolman, S. D. Ittel, A. D. English and J. P. Jesson, *J. Am. Chem. Soc.*, 1979, **101**, 1742.

9 M. E. van der Boom, S. Y. Liou, Y. Ben-David, L. J. W. Shimon and D. Milstein, *J. Am. Chem. Soc.*, 1998, **120**, 6531.

10 *(a)* P. Lara, M. Paneque, M. L. Poveda, V. Salazar, L. L. Santos and E. Carmona, *J. Am. Chem. Soc.*, 2006, **128**, 3512; *(b)* L. L. Santos, K. Mereiter and M. Paneque, *Organometallics*, 2013, **32**, 565.

11 *(a)* J. Choi, Y. Choliy, X. W. Zhang, T. J. Emge, K. Krogh-Jespersen and A. S. Goldman, *J. Am. Chem. Soc.*, 2009, **131**, 15627; *(b)* S. Kundu, J. Choi, D. Y. Wang, Y. Choliy, T. J. Emge, K. Krogh-Jespersen and A. S. Goldman, *J. Am. Chem. Soc.*, 2013, **135**, 5127.

12 M. C. Haibach, N. Lease and A. S. Goldman, *Angew. Chem. Int. Ed.,* 2014, **53**, 10160.

13 G. A. Edouard, P. Kelley, D. E. Herbert and T. Agapie, *Organometallics,* 2015, **34**, 5254

14 R. J. Trovitch, E. Lobkovsky, M. W. Bouwkamp and P. J. Chirik, *Organometallics*, 2008, **27**, 6264

15 K. A. Manbeck, S. Kundu, A. P. Walsh, W. W. Brennessel and W. D. Jones, *Organometallics*, 2012, **31**, 5018.

16 R. A. Widenhofer and S. L. Buchwald, *J. Am. Chem. Soc.*, 1998, **120**, 6504.

17 *(a)* J. F. Hartwig, *Angew. Chem. Int. Ed.,* 1998, **37**, 2046; *(b)* J. P. Stambuli, Z. Weng, C. D. Incarvito and J. F. Hartwig, *Angew. Chem. Int. Ed.,* 2007, **46**, 7674; *(c)* S. L. Marquard and J. F. Hartwig, *Angew Chem. Int. Ed.,* 2011, **50**, 7119; *(d)* C. S. Sevov and J. F. Hartwig, *J. Am. Chem. Soc*., 2013, **135**, 9303.

18 *(a)* K. Koo and G. L. Hillhouse, *Organometallics,* 1998, **17**, 2924; *(b)* P. T. Matsunaga, G. L. Hillhouse and A. l. Rheingold, *J. Am. Chem. Soc.,* 1993, **115**, 2075.

19 J. R. Khusnutdinova, P. Y. Zavalij and A. N. Vedernikov, *Organometallics,* 2007, **26**, 3466.

20 M. C. Haibach, C. Guan, D. Y. Wang, B. Li. N. Lease, A. M. Stefens, K. Krogh-Jespersen and A. S. Goldman, *J. Am. Chem. Soc.,* 2013, **135**, 15062.

21 N. A. Jasim, R. N. Perutz, B. Procacci and A. C. Whitwood, *Chem. Commun.*, 2014, **50**, 3914.

22 M. J. Ingleson, M. F. Mahon and A. S. Weller, *Chem. Commun.*, 2004, 2398.

23 M. A. Ortuño, S. Conejero and A. Lledós, *Beilstein J. Org. Chem.*, 2013, **9**, 1352.

24 M. A. Ortuño, P. Vidossich, S. Conjero and A. Lledós, *Angew. Chem. Int. Ed.*, 2014, **53**, 14158.

25 M. A. Ortuño, P. Vidossich, G. Ujaque, S. Conejero and A. Lledós, *Dalton Trans.*, 2013, **42**, 12165.

26 M. Feliz, Z. Freixa, P. W. N. M. van Leeuwen and C. Bo, *Organometallics*, 2005, **24**, 5718.

27 *(a)* F. M. Bickelhaupt, T. Ziegler and P. v. R. Schleyer, *Organometallics,* 1995, **14**, 2288; *(b)* C. Gourlaouen, G. Ujaque, A. Lledós, M. Medio-Simón, G. Asensio and F. Maseras, *J. Org. Chem.*, 2009, **74**, 4049; *(c)* C. Mollar, M. Besora, F. Maseras, G. Asensio and M. Medio-Simón, *Chem. Eur. J.*, 2010, **16**, 13390; *(d)* M. Besora, C. Gourlaouen, B. Yates and F. Maseras, *Dalton Trans.*, 2011, **40**, 11089.

28 As a rough estimate of the process, the radical ions $[Pt(I)L_2]^{\cdot+}$ **1·+** and $[ArOMe]^{\cdot-}$ **b·–** were found at 69.2 kcal mol^{-1} above reactants **1** and **b**.

29 *(a)* M. Ahlquist, P. Fristrup, D. Tanner and P. O. Norrby, *Organometallics*, 2006, **25**, 2066; *(b)* C. L. McMullin, J. Jover, J. N. Harvey and N. Fey, *Dalton Trans.*, 2010, **39**, 10833; *(c)* K. Vikse, T. Naka, J. S. McIndoe, M. Besora and F. Maseras, *ChemCatChem*, 2013, **5**, 3604.

30 P. Vidossich, G. Ujaque and A. Lledós, *Chem. Commun.*, 2014, **50**, 661.

31 No computational studies for Pt(0)-mediated S_N2 reactions have been found. For Pt(II) derivatives see for instance: *(a)* T. Kégl and L. Kollár, *J. Organomet. Chem.*, 2007, **692**, 1852; *(b)* S. Hayaki, D. Yokogawa, H. Sato and S. Sakaki, *Chem. Phys. Lett.*, 2008, **458**, 329; *(c)* W.-G. Liu, A. V. Sberegaeva, R. J. Nielsen, W. A. Goddard III and A. N. Vedernikov, *J. Am. Chem. Soc.*, 2014, **136**, 2335.

32 The closely related $[PtMe(P^iPr_3)_2]^+$ complex shows a γ-agostic interaction, Pt···H_{ag} = 2.24 Å and Pt···C_{ag} = 2.859 Å. reference 22.

33 *(a)* W. Baratta, S. Stoccoro, A. Doppiu, E. Herdtweck, A. Zucca and P. Rigo, *Angew. Chem., Int. Ed.*, 2003, **42**, 105; *(b)* H. Braunschweig, K. Radacki and K. Uttinger, *Chem.–Eur. J.*, 2008, **14**, 7858; *(c)* S. H. Crosby, G. J. Clarkson and J. P. Rourke, *J. Am. Chem. Soc.*, 2009, **131**, 14142; *(d)* O. Rivada-Wheelaghan, B. Donnadieu, C. Maya and S. Conejero, *Chem.–Eur. J.*, 2010, **16**, 10323; *(e)* J. Campos, R. Peloso and E. Carmona, *Angew. Chem., Int. Ed.*, 2012, **51**, 8255.

34 The process from **1b·OAr** to **1b+** and ArO^- is actually quite endothermic (ΔΔH = +11.7 kcal mol^{-1}) but turns slightly exergonic (ΔΔG = –2.1 kcal mol^{-1}) due to the substantial entropic contributions that arise from separating two species.

35 *(a)* M. D. Butts, B. L. Scott and G. K. Kubas, *J. Am. Chem. Soc.*, 1996, **118**, 11831; *(b)* J. C. Thomas and J. C. Peters, *J. Am. Chem. Soc.* 2001, **123**, 5100; *(c)* J. C. Thomas and J. C. Peters, *J. Am. Chem. Soc.* 2003, **125**, 8870.

36 (a) N. A. Jasim, R. N. Perutz, A. C. Whitwood, T. Braun, J. Izundu, B. Neumann, S. Rothfeld anmd H.-G. Stammler, *Organometallics,* 2004, **23**, 6140; (b) A. Nova, S. Erhardt, N. A. Jasim, R. N. Perutz, S. A. Macgregor, J. E. McGrady and A. C. Whitwood, *J. Am. Chem. Soc.*, 2008, **130**, 15499.

37 H. B. Bürgi and J. D. Dunitz, *Acc. Chem. Res.,* 1983, **16**, 153.

38 *(a)* A. P. Bento and F. M. Bickelhaupt, *J. Org. Chem.*, 2008, **73**, 7290; *(b)* Q.-G. Li and Y. Xue, *J. Phys. Chem. A*, 2009, **113**, 10359.

39 J. D. Smith and J. D. Oliver, *Inorg. Chem.,* 1978, **17**, 2585.

40 R. G. Pritchard, A. J. Adamson, R. E. Banks. W. Jondi and A. E. Tipping, *Acta Crystallogr. Sect. C: Cryst. Struct. Commun.* 1991, **47**, 1124.

41 A. S. Batsanov and G. Sanford, structure VECTIH in The Cambridge Structural Database C. R. Groom, I. J. Bruno, M. P. Lightfoot and S. C. Ward, *Acta Crystallogr. Sect. B: Struct. Sci.* 2016, **72**, 171.

42 T. Braun, S. Rothfeld, V. Schorlemer, A. Stammler and H.-G. Stammler, *Inorg. Chem. Commun.*, 2003, **6**, 752.

43 T. S. Attig and H. C. Clark, *J. Organomet. Chem.,* 1975, **94**, C49.

44 B. E. Mann and A. Musco, *J. Organomet. Chem.,* 1979, **181**, 439.

45 We have also investigated the reaction of $Pt(PCyp_3)_2$ with 2,3,5,6-tetrafluoro-4-allyloxypyridine and shown that it yields an analogous product to that formed with $Pt(PCy_3)_2$ and proceeds at a similar rate.

46 C.-H Wu, B. Galabov, J. I.-C. Wu, S. Ilieva, P. von R. Schleyer and W. D. Allen, *J. Am. Chem. Soc.,* 2014, **136**, 3118.

47 C. J. Cramer and D. G. Truhlar, *Phys. Chem. Chem. Phys.*, 2009, **11**, 10757.

48 Y. Zhao and D. G. Truhlar, *Theor. Chem. Acc.*, 2008, **120**, 215.

49 S. E. Wheeler and K. N. Houk, *J. Chem. Theory Comput.,* 2010, **6**, 395.

50 Gaussian 09 (Revision D.01): M. J. Frisch et al. Gaussian, Inc., Wallingford CT, 2011.

51 *(a)* Y. Zhao and D. G. Truhlar, *Acc. Chem. Res.*, 2008, **41**, 157; *(b)* Y. Zhao and D. G. Truhlar, *Chem. Phys. Lett.*, 2011, **502**, 1.

52 D. Andrae, U. Haeussermann, M. Dolg, H. Stoll and H. Preuss, *Theor. Chim. Acta*, 1990, **77**, 123.

53 A. W. Ehlers, M. Bohme, S. Dapprich, A. Gobbi, A. Hollwarth, V. Jonas, K. F. Kohler, R. Stegmann, A. Veldkamp and G. Frenking, *Chem. Phys. Lett.*, 1993, **208**, 111.

54 *(a)* W. J. Hehre, R. Ditchfield and J. A. Pople, *J. Chem. Phys.,* 1972, **56**, 2257; *(b)* M. M. Francl, W. J. Pietro, W. J. Hehre, J. S. Binkley, M. S. Gordon, D. J. DeFrees and J. A. Pople, *J. Chem. Phys.*, 1982, **77**, 3654.

55 T. Clark, J. Chandrasekhar, G. W. Spitznagel and P. v. R. Schleyer, *J. Comput. Chem.*, 1983, **4**, 294.

56 A. V. Marenich, C. J. Cramer and D. G. Truhlar, *J. Phys. Chem. B*, 2009, **113**, 6378.

57 A. V. Marenich, S. V. Jerome, C. J. Cramer and D. G. Truhlar, *J. Chem. Theory Comput.*, 2012, **8**, 527.
58 Linden, H. B. *Eur. J. Mass Spectrom.,* 2004, **10**, 459.
59 T. Yoshida and S. Otsuka, *Inorg. Synth*., 1979, **19**, 101.
60 O. V. Dolomanov, L. J.Bourhis, R. J. Gildea, J. A. K. Howard and H. Puschmann, *J. Appl. Crystallogr.,* 2009, **42**, 339.
61 G. M. Sheldrick, *Acta Crystallogr., Sect. A: Found. Crystallogr.* 2008, **64**, 112.

Table of Contents Entry

DFT calculations demonstrate that Pt(0) bis(phosphine) complexes react with Ar^F-O-Me via an S_N2 mechanism to activate the O-CH_3 bond; experimental support is provided by reaction of $Pt(PCy_3)_2$ with 2,3,5,6-tetrafluoro-4-allyloxypyridine to form an aryloxide salt of $[Pt(\eta^3\text{-allyl})(PCy_3)_2]^+$.